

Formulation Development and Evaluation of Febuxostate Nanoemulsion Emulsion for the Treatment of Gout

Mr. Vinod Bapurao Landge^{*1}, Dr. Santosh R Jain¹, L. D. Hingane¹
¹Aditya pharmacy college Beed (Maharashtra)

Submitted: 01-07-2022

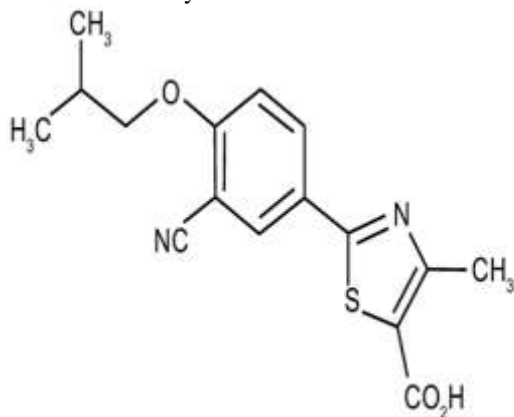
Accepted: 14-07-2022

ABSTRACT: The aim of present research was to design and develop Nanoemulsion of Febuxostat for solubility enhancement. Febuxostat is a non-purine selective inhibitor of xanthine oxidase. It belongs to BCS class II i.e. poorly soluble and highly permeable drug. Due to its poor solubility, it is incompletely absorbed after oral dosing and bioavailability varies among individuals. Therefore, to overcome these shortcomings nanoemulsions have been designed. Nanoemulsion was formulated by high speed homogenization technique using isopropyl myristate as oil, tween 80 and span 80 were selected as surfactant. The formulations were evaluated for droplet size, zeta potential, drug content. The optimized formulation contains droplet size 358.5nm and zeta potential -29.1mv. In-vitro dissolution study of nanoemulsion showed 42.37 % release within 6hrs. Hence, it is concluded that nanoemulsion enhances the solubility of Febuxostat.

Keywords: Febuxostat, Nano emulsion, isopropyl myristate, zeta potential.

I. INTRODUCTION¹⁻¹⁰

Febuxostat denoted as FBX is a non purine selective inhibitor of xanthine oxidase/xanthine reductase. The chemical name of FBX is 2-[3-cyano-4-(2-methyl propoxy) phenyl]-4-methyl, 3-thiazole-5-carboxylic acid.



Chemical structure of Febuxostat

It is indicated for the long-term management of hyperuricemia in patients with gout. It belongs to BCS class II with low solubility and high permeability. Because of low solubility the bioavailability of the drug is hampered and it also undergoes enzymatic degradation in intestine as well as in liver. Food interferes with the absorption of drug and decreases the C_{max} to 38-49%. Thus, it has undesirable dissolution profile and poor bioavailability following oral administration. Poor water soluble drugs present significant challenges during dosage form designing due to their inadequate solubilization in digestive fluids. Most of the newly discovered drugs receive little or no aqueous solubility as a challenge for the successful formulation development and commercialization of new drugs in the pharmaceutical industry. The bioavailability of a drug is a function of dissolution rate of the drug which is controlled by the surface area of the drug. In the category of poorly soluble drugs the change in surface area of the drug will show considerable changes in the solubility and dissolution of the drug. Febuxostat belongs to BCS class II i.e. poorly soluble and highly permeable drug. Due to poor solubility, it is incompletely absorbed after oral dosing and bioavailability varies among individuals. To overcome these shortcomings novel drug delivery system (NDDS) plays a crucial role. Nano emulsions have been widely used especially in dermatology. They are capable to incorporate a variety of hydrophilic and hydrophobic drugs, to enhance the accumulation of drug at the administration site and to reduce side effects. They are considered to be in the range of 100 nm to 1000nm. Various effects such as surface area and area to volume ratio and many other physical properties get magnified when reduced to nanoscale. Most of the current research works in almost all technical and biomedical fields is based on nano size. Nano emulsions are thermodynamically stable transparent (translucent) dispersions of oil and water stabilized by an

interfacial film of surfactant molecules having a droplet size of less than 1000 nm. The optically clear and low-viscous formulation with enhanced solubility and minimum droplet size diameter would pose a definite promise in improving the significance of poorly soluble drug. So, the objective of the present research work was to formulate Nano emulsion of Febuxostat for improving the solubility and bioavailability of drug.

II. MATERIAL AND METHODS:

Materials

Febuxostat was generously gifted by Sun Pharma Mumbai, isopropyl myristate, span 80, tween 80 were procured from SD fine chemicals and all other chemicals and solvents were of analytical grade.

Methods

Determination of organoleptic properties

The physical identification of Febuxostat was done by checking its physical appearance i.e. colour, nature and physical state. Weighed quantity of Febuxostat as drug was taken and viewed in well illuminated place.

Determination of Melting point

Melting point of the drug was determined by using capillary method. Drug was filled into capillary tube by sealing its one end at the height of 3 mm from the closed end. The capillary was introduced into the digital melting point apparatus and the point at which the drug starts melting was noted until the entire samples get melted.

Identification of drug by FTIR

Fourier transforms infrared spectral spectroscopy (FTIR) the pure drug was mixed with IR grade potassium bromide in a ratio of (1:100) and pellets were prepared by applying 10 metric ton of pressure in shimadzu hydrophilic press. The pellets were then scanned over range of 4000-400 cm⁻¹ in FTIR spectrometer. FTIR spectrum of Febuxostat showed the presence of the peaks which complies with the reference spectra.

Preparation of Standard Calibration Curve of Febuxostat

10 mg of drug (Febuxostat) was accurately weighed from calibrated digital weighing balance and was transferred to 100 ml volumetric flask. Small quantity of methanol was added to dissolve the drug. The volume was made up to 100 ml using methanol to prepare stock solution of 100 µg/ml. From the stock solution 0.2, 0.4, 0.6, 0.8, 1.0 ml of solution was pipetted into 10 ml volumetric flasks and volume was made up to 10 ml to form concentrations of 2, 4, 6, 8, 10 µg/ml with phosphate buffer. The absorbance was measured with the help of UV Spectrophotometer at 318 nm by taking phosphate buffer as reference solution. All the studies were done in triplicate (n=3) with the same instrument.

Determination of solubility of various solvents (oil, surfactants)

In this excess amount of drug (Febuxostat) was taken and dissolved in various excipients used in the study. The solutions were sonicated for 1hr at room temperature and maintained at 25°C for 48 hrs on an orbital shaker Orchid, Mumbai. Then this was filtered through a 0.22µm nylon membrane filter. These were suitably diluted and analyzed, spectrophotometrically (UV/Vis spectrophotometer, Elico), for the dissolved drug at 318 nm. All trials were performed in triplicate.

PREPARATION OF NANOEMULSIONS:

Nanoemulsion of Febuxostat was prepared using solvent evaporation followed by probe sonication emulsification technique. In detail, the aqueous phase was prepared by dispersing Captex 200 P (1.71 mL) & Egg lecithin (1.77 mL) in distilled water with continuous stirring. The organic phase was prepared by adding different amounts of Tween 80 into Captex oil. The drug was dissolved in this oil and surfactant mixture with continuous stirring. The aqueous phase and the oil phase were heated separately at 60-70°C with stirring. The oil phase was then homogenized into aqueous phase using a high-speed homogenizer (Ultraturrax, IKA-T23) at 10,000 rpm for 20 min at 50-60°C. Then emulsion was transferred to probe sonicator apparatus and the temperature was maintained between 25°C during [1].

Table 1: The coded and actual values of the variables used in the full factorial design of FBX-NEs

Independent Variables	Actual and coded values	
	Low (-1)	High (+1)
X ₁ = Conc. of Oil	0.5	1
X ₂ = Conc. of S-mix	0.5	1

Optimization of the ingredients using a full factorial design

Table is the 3² full factorial design with the content of lipid (X1), polymer (X2) as independent variables or PS, ZP, PDI, and EE as responses. The result of the experimental design was analyzed using Statistical software Design-Expert® Version 7.0.0. Each response coefficient was studied for its statistical significance at a 95% confidence level. The P-value of probe > F^{**} less than 0.05 indicates that model terms are significant and greater than 0.05 indicates that model terms are insignificant and should be removed from analysis to generate the reduced model. All independent variables, their levels along

with actual and coded values of these variables are shown in Table 2. Whereas mean particle size of FBX-NEs use as (Y1), ZP as (Y2), PDI as (Y3) & %EE as Y4 were selected as response parameter as the dependent variables. Using this design, we were able to choose the best model among the linear, two-factor interaction model and quadratic model due to the analysis of variance (ANOVA) F-value by using Statistical software Design-Expert® Version 7.0.0 was employed for statistical analysis and graph plotting. The effect of independent variables on the responses was calculated by

Table 2: Formulations of NEs loaded with FBX by 3² simple full factorial design

Run	X1(mL)	X2(mL)
F1	2.50(+1)	2.25(-1)
F2	1.50(+1)	2.25(+1)
F3	2.00(-1)	2.00(+1)
F4	1.50(+1)	2.25(-1)
F5	1.50(-1)	1.75(-1)
F6	2.00(+1)	1.75(-1)
F7	1.50(-1)	2.00(-1)
F8	2.50(+1)	1.75(+1)
F9	2.50(+1)	2.00(-1)

X1 (mL) = Oil (high level-1.0, low level-0.5), X2 (mL) = S-mix (surfactant & co-surfactant) concentration (high level-1.0, low level-0.5).

Characterization of Nanoemulsion

Characterization of nano-emulsions is of most importance in order to ensure the production of emulsions which fall within the desired droplet size range, viscosity and charge and are stable with time. Several techniques have been developed to characterize emulsions such as particle size analysis, polydispersity index and zeta potential

determination, differential scanning calorimetry. Some of these methods will be highlighted below.

1. Thermodynamic stability studies: The formulations were subjected to different thermodynamic stability tests.

a) Heating cooling cycle: Three cycles between the temperature 4°C and 45°C with storage at each temperature not less than 48 hrs was studied. Those formulations, which were stable at these temperatures, were subjected to centrifugation test.

b) Centrifugation: formulations which were stable in the above test were centrifuged at 3600 rpm for 30min. Those formulations that did not show any

phase separation were taken for freeze thaw stress test.

c) Freeze thaw cycle: Between – 18°C and +25°C three freeze thaw cycles with storage at each temperature for not less than 48 h was done for the formulations.

2. Drug content: in this 2 ml of Nano emulsion was taken in 10 ml volumetric flask and the volume was made up to 10 ml using methanol. 1ml of stock solution was diluted to 10 ml with phosphate buffer pH 6.0 phosphate buffer which was further diluted to give a final concentration of 10 µg/ml (10ppm) solution. Percent drug content was calculated spectrophotometrically at 318 nm.

3. Particle size determination: Particle size of emulsion can be determined using several techniques. Some of the major techniques are hydrodynamic chromatography, photon correlation spectroscopy, spectroturbidimetry, field flow fractionation, sensing zone, electron microscopy and sedimentation.

4. Zeta Potential: Determination Zeta potential is a measurement of surface potential. The magnitude of zeta potential gives an indication of potential stability of an emulsion. Zeta potential is an important parameters in determining the stability of an emulsion and other colloidal dispersion, zeta

potential larger than about 25mV is typically required to stabilize a colloidal system. Zeta potential is determined by a number of factors, such as the particle surface charge density, the concentration of counter ions in the solution, solvent polarity and temperature. Zeta potential can be determined using the Malvern Zeta sizer or the Nicomp particle sizer. Zeta potential is determined by electrophoretic light scattering (ELS). The smoluchowski equation can be used to compute the zeta potential from electrokinetic mobility μ . $\mu = \zeta \epsilon / \eta$equation. Where ϵ is the permittivity and η the viscosity of the liquid used

5. Dissolution studies of Nanoemulsions: Dissolution studies for febuxostat Nano emulsions were performed in pH 6 phosphate buffer using USP dissolution test apparatus with a paddle stirrer. The paddles were allowed to rotate at a speed of 75 rpm. The dissolution medium was maintained at a temperature of 37±0.5°C and the samples were withdrawn for every 1hr. The volume of withdrawal samples were replaced by fresh dissolution medium in order to keep the volume of dissolution medium constant. Then the withdrawal samples were checked for absorbance at 318 nm using UV-Visible spectrophotometer.

III. RESULTS AND DISCUSSIONS:

Physical appearance: Physical appearance of febuxostat

Test	Specification	Observation
Nature	Amorphous	Amorphous
Color	White	White
Physical state	Solid powder	Solid powder

Melting point: analysis Melting range of febuxostat was found to be 238-239°C

Identification of drug by FTIR: Fourier transformed infrared (FTIR) spectra of FBX was taken by using the KBr disk method. The

obtained IR spectra of FBX given in Fig. Observed peaks of the FBX are shown in Table. which are similar to the standard IR spectra of drug reported in the literature.

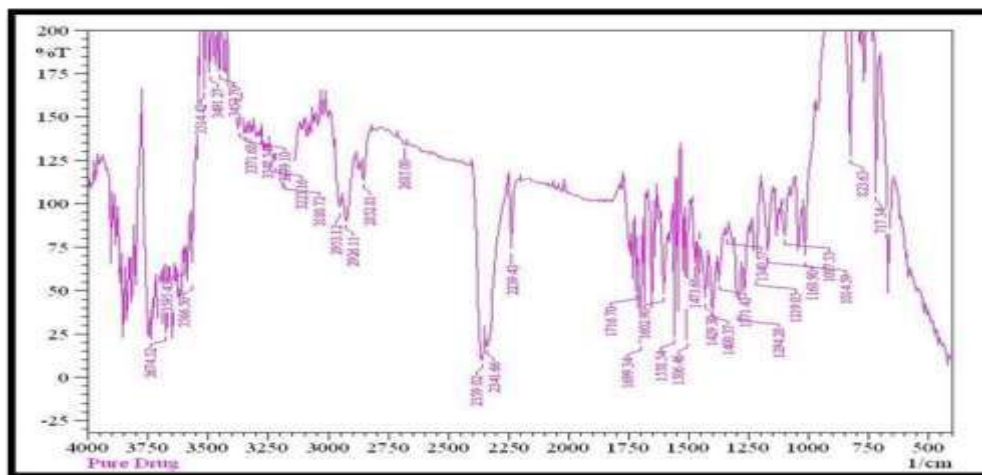


Table1:ObservedpeakofFBX

Range	Observedpeakes	Functional Group
3300-2500	2953.12	COOH
2260-2222	2239.43	C=N
1780-1650	1699.34	C=O
1400-1600	823.63	Thiazolering
1275-1200	1219.05	Alkylarylerher

STANDARD CALIBRATION CURVE

Standard calibration curve of Febuxostat (FBX) in methanol
 Graph of absorbance Vs concentration was plotted

and found to be linear over the range of 2-12 µg/ml indicating its compliance with Beer's and Lambert's law. Results are shown in Table 8.4 and Fig.

Table3:Standard calibration curve of (FBX) in methanol

Concentration (µg/mL)	Absorbance
0	0.000
2	0.123
4	0.282
6	0.422
8	0.545
10	0.791
12	0.123

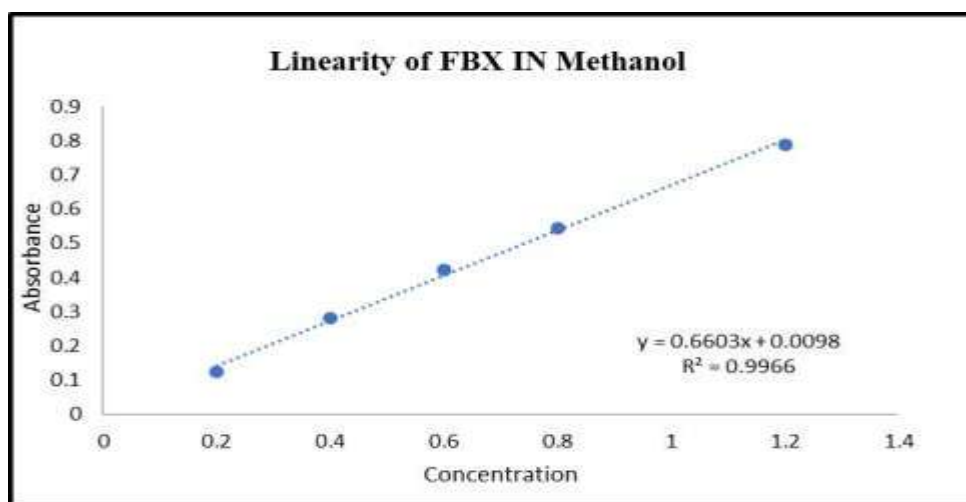


Figure 3: Standard calibration curve of Febuxostat (FBX) in methanol

SOLUBILITY STUDY:

Solubility is the property of a solid, liquid, or gaseous chemical substance called solute which is to be dissolved in a solid, liquid, or gaseous solvent to form a homogeneous solution of the solute in the solvent. The solubility of a substance fundamentally depends on the solvent used as well as on temperature and pressure. The extent of the solubility of a substance in a specific solvent is measured as the saturation concentration where adding more solute does not increase its concentration in the solution. The solubility of Febuxostat (FBX) was assessed by the shake flask method. Briefly, an excess amount of Febuxostat was added to

1 mL of each sample (oil/surfactant) in a test tube and vortex up to 10 to 15 min at the vortex and then stay for 12 hrs. After that sample was centrifuged at 10,000 rpm for 10 min to settle undissolved drugs. An aliquot of the supernatant was suitably diluted with methanol and the concentration of Febuxostat was determined spectrophotometrically. The solubility data was reported in Table 12 and solubility of Febuxostat in different solvents was shown in Fig. 4.

a) Pseudo ternary Phase Diagram:

Preparation of phase diagram of the pseudo ternary phase diagrams of oil, surfactant, co-surfactant, and water was developed using the aqueous titration method to obtain the NE region. Furthermore, to optimize the ratio of surfactant and co-surfactant, different ratios

of Smix (1:1, 2:1, 3:1, and 4:1) were taken. For each, phase diagram, the ratio of oil to the Smix were varied as 1:9, 1:8, 1:7, 1:6, 1:5, 1:3.5, 1:3, 1:2, 2:8, 3:7, 4:6, 5:5, 6:4, 7:3, 8:2 and 9:1.

Water was added drop-wise to each Oil-Smix mixture under vigorous mixing. Based on the above results, Captex 200 P, Tween-80 as a surfactant, and Lipoid E 80 as a co-surfactant was chosen as candidates in preparation of NE. These excipients were also found miscible with each other. The pseudo-ternary phase figures of several S-mix ratio is presented in Fig 10. Tween 80 and Lipoid E80 were selected to obtain the S-mix. The colored spots represent the NE area. Four pseudo-ternary phase systems were created, in which the Smix was made at different mass ratios (1:1, 2:1, 3:1, and 4:1). Fig. 8.8 represents that Smix 1:1 has a minimum NE area, whereas S-mix 2:1 created the maximum NE area. As we decrease the concentration of surfactant, from Smix 4:1 to Smix 2:1, a higher NE area was observed. It might be due to the higher HLB value of Tween-80 (HLB-15), and with an addition in the quantity of Tween-80, the HLB of the system also increases. For the development of ternary phase diagrams, the Smix ratio below 4:1 was not selected because as we decreased this ratio the NE region also decreased. Furthermore, the S-mix ratio above 2:1 was also not selected because it also produces a ternary phase diagram with a lesser NE region. Based on the pseudo-ternary phase diagram, a 2:1 ratio of Tween 80 and Lipoid E 80 was confirmed owing to its more oil solubilizing potential. For the optimization purpose, the “minimum” quantity of

Smix was applied as a constraint on the remaining five NEs. Based on the constraint applied, it was found to be the optimized formulation that was further subjected to characterization.

Table4:TernaryphaseaqueousTitration resultsinS-mixRatio1:1

a)S-mix(1:1)

Sr no.	Volof oil	VolofSmix	Volofwater	water(% w/w) w1	S-mix(% w/w) w2	Oil(% w/w) w3
1	0.1	0.9	1.5	29.18	35.01	3.57
2	0.2	0.8	1.8	46.89	43.51	9.5
3	0.3	0.7	2.3	56.76	36.48	9.07
4	0.4	0.6	2	51	28	21
5	0.5	0.5	5	33.69	4.3	61.99
6	0.6	0.4	0.3	13	55	31
7	0.7	0.3	0.4	16.4	60.95	22.63
8	0.8	0.2	0.3	12.71	72.03	15.25
9	0.9	0.1	0.2	8.73	83.4	7.86

Table5:TernaryPhaseaqueous titration resultsin smix2:1

b)Smix(2:1)

Sr no.	Vol.of oil	Volof Smix	Volof water	Water (% w/w) w1	Smix(% w/w) w2	Oil(% w/w) w3
1	0.1	0.9	6.5	95.72	1.62	2.65
2	0.2	0.8	5.5	79.64	4.42	15.92
3	0.3	0.7	5	74.07	21.93	36.31
4	0.4	0.6	1	33.33	42.33	24.33
5	0.5	0.5	0.6	37.97	4.05	58.22
6	0.6	0.4	0.3	13.33	37.77	48.88
7	0.7	0.3	0.2	9.47	29.85	60.66
8	0.8	0.2	0.2	9.56	20.09	70.33
9	0.9	0.1	0.1	4.71	10.04	79.23

Table6:TernaryphaseaqueoustitrationinS-mix(3:1)

c)Smix(3:1)

--

Srno.	Vol of oil	Vol of Smix	Vol of water	Water (% w/w)w1	Smix(% w/w)w2	Oil (% w/w)w3
1	0.1	0.9	5	70.52	26.93	2.53
2	0.2	0.8	0.8	27.53	59.4	12.48
3	0.3	0.7	0.4	22.22	65.77	12
4	0.4	0.6	0.3	16.66	52.91	30.41
5	0.5	0.5	0.3	12.19	63	28.04
6	0.6	0.4	0.5	13.33	48.88	7.3
7	0.7	0.3	0.2	20.74	26.14	53.11
8	0.8	0.2	0.2	9.56	20.09	70.33
9	0.9	0.1	0.2	9.7	10.19	80.09

Table 7 Ternary phase equilibrium titration result smix ratio 4:1

d) Smix(4:1)

Srno.	Vol of oil	Vol of Smix	Vol of water	Water (% w/w)w1	Smix (% w/w)w2	Oil (% w/w)w3
1	0.1	0.9	3.5	62.61	34.16	3.22
2	0.2	0.8	0.2	8.84	75.22	15.92
3	0.3	0.7	0.6	25.53	62.97	11.48
4	0.4	0.6	0.5	20	50.8	29.2
5	0.5	0.5	0.3	13.15	46.66	40.35
6	0.6	0.4	0.4	20.2	42.92	36.86
7	0.7	0.3	0.4	17.31	27.27	55.41
8	0.8	0.2	0.3	12.76	17.02	7.21
9	0.9	0.1	0.2	9.75	10.24	80.47

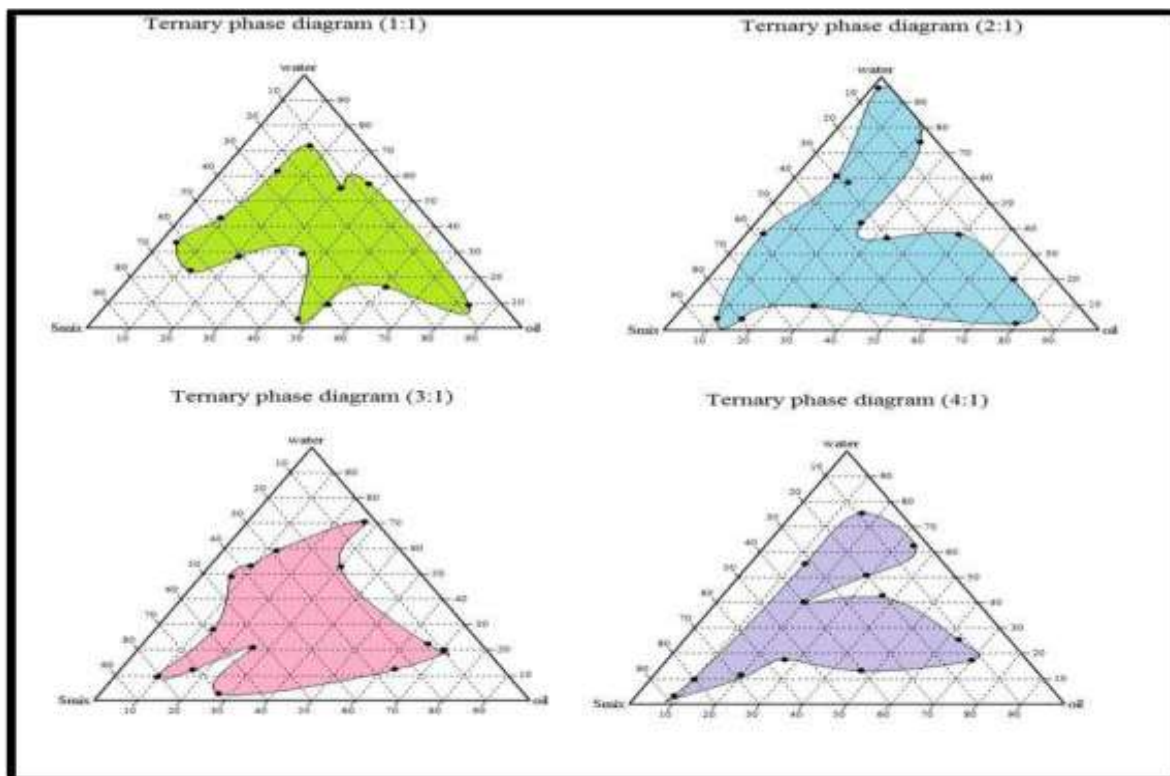


Figure 4: Pseudo-ternary phase diagrams of different S-mix ratios.

Particle size and Polydispersity index of FBX-NE

The major objective of using general optimal design was to determine the levels of the two factors i.e. oil and surfactant concentration (1.71 mL) (X₁) and Surfactant, Co-surfactant Concentration (1.77 mL) (X₂) which produce the NEs with minimum particle size and maximum entrapment efficiency. The particle size of the NEs is a crucial factor because it determines the rate and extent of drug release as well as drug absorption. The smaller droplet size provides a larger interfacial surface area for drug absorption. Also, it was suggested that the smaller droplet size permit a faster release rate. Also, it has been reported that the smaller particle size of the nanoemulsion droplets may lead to more rapid absorption and improve bioavailability. Also, PDI measures the width of particle size distribution. If PDI is lower than 0.1, it might be associated with high homogeneity in the particle population, whereas high PDI values suggest a broad size distribution. The particle size

and polydispersity index (PDI) of the fabricated batches were in the range of 92.2 to 79.2 nm, and 0.383 to 0.316 respectively. It has been previously reported that several particles of mean diameter around 0.3 and 1.0 μm are preferably absorbed by the payer's patches (which drains its content into the lymphatic system) in comparison to particles of 3.0 μm. The particle size obtained in the present study is within the size range (92.2 to 79.2 nm) required for efficient lymphatic uptake, therefore, it may be expected that the size is acceptable and would not be a limiting factor in the lymphatic uptake of the prepared nanoemulsions. Sizes of FBX-NEs, with different percentages of Captex 200 P, Tween 80, and Lipoid E 80 are shown along with the Polydispersity index (PDI) in Table 21. The particle size and Polydispersity index (PDI) of the optimized FBX-NEs was found to be 74.88 nm and 0.308 respectively as seen in Figure 5.

Table 5: Particlesize, PDI, Zetapotential and % EE of Febuxostat loaded NEs

Run	X1(mL)	X2(mL)	PS Y1 (nm)	ZP Y2	PDI Y3	EE Y4(%)
F1	2.50(+1)	2.25(-1)	90.1	-32.2	0.323	82.5
F2	1.50(+1)	2.25(+1)	85.2	-32.5	0.332	78.2
F3	2.00(-1)	2.00(+1)	79.2	-26.3	0.358	85.3
F4	1.50(+1)	2.25(-1)	87.1	-25.6	0.316	86.2
F5	1.50(-1)	1.75(-1)	86.4	-29.1	0.334	84.3
F6	2.00(+1)	1.75(-1)	88.5	-28.3	0.359	87.6
F7	1.50(-1)	2.00(-1)	80.4	-29.6	0.345	79.7
F8	2.50(+1)	1.75(+1)	92.2	-35.2	0.383	74.2
F9	2.50(+1)	2.00(-1)	81.2	-32.1	0.312	75.5

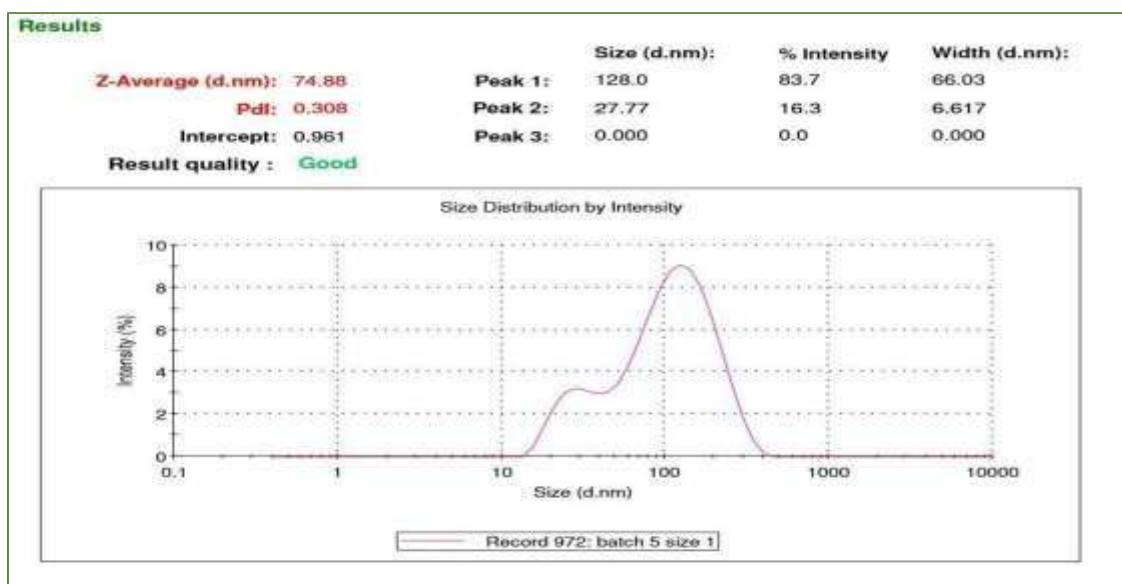


Figure 6: Droplet diameters size graph of optimized formulation

Conductivity Test

The o/w nanoemulsion passes the conductivity test due to water in the continuous phase while w/o nanoemulsion vice-versa. The resultant nanoemulsion is of o/w type as optimized nanoemulsion shown the conductivity with a value of 167.66 ± 0.57 mS (mean \pm SD, n=3).

From batch F, average droplet size increases which could be attributed to the interfacial disruption elicited by enhanced water penetration into the oil droplets mediated by the high surfactant concentration and leading to the ejection of oil droplets into the aqueous phase. Varying polydispersity values show that good droplet distribution had occurred in

some batches while in some droplet distribution i.e. PDI > 0.2 which is quiet, not suitable for nanoemulsion. Moreover, it can be seen that formulation F12 had required. Amount of drug-loaded in nanoemulsion passing thermodynamic stability test. So, the formulation F was considered to be optimized as the droplet size (± 0 nm) (mean \pm SD, n=3) was minimum as a comparison with other formulation. The polydispersity index of formulation F is lowest having a value of \pm (mean \pm SD, n=3). Since the diameter of the dispersed oil droplets of the optimized nanoemulsion (F12) was much smaller than the 100 nm, such droplets are considered to be suitable for intranasal administration to achieve

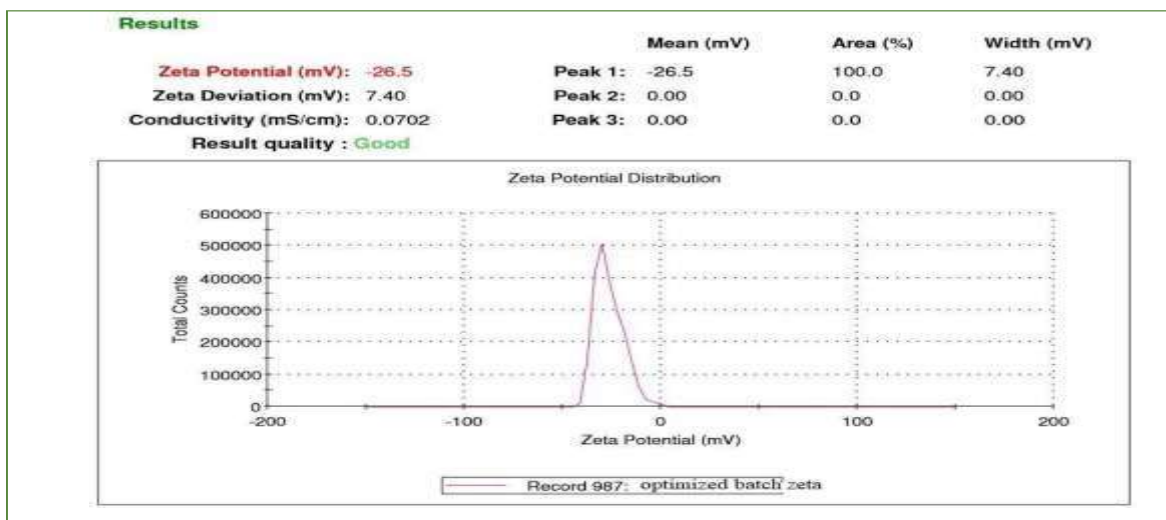
brain targeting. The droplet size of the nanoemulsion is an important factor as this determines the rate and extent of drug release as well as absorption.

Zeta potential determination

The zeta-potential of the optimized FBX-NEs was found to be -26.5 as seen in Figure 8.16. It possesses negative surface charges due to the negatively charged Tween 80. Also, both surfactant (Tween 80) and co-surfactant (Lipoid E 80-Egg Lecithin) were also negatively charged. It is currently admitted that zeta potentials under -30 mV, are optimum and less than (-60) mV, are required for full electrostatic stabilization. Electrostatic surfactants are known to impart favorable electrical potential to nanoparticles leading to higher zeta potential. However, higher concentrations of these surfactants decrease the zeta potential of nanoparticles due to a reduction in the thickness of the diffuse layer. Consequently, it has been proposed that to impart practical electrical properties on nanoemulsions, the electrostatic surfactants should be used in conjunction with stearic surfactants. In general, particles could be dispersed stably when the absolute value of zeta potential is above 30 mV due to the electric repulsion between particles. We found zeta potential values of the NEs in the range of 26.2- to -25.6 mV. This implies that the FBX-NEs prepared using solvent evaporation followed by probe sonication emulsification method would be a physically stable system.

icles leading to higher zeta potential. However, higher concentrations of these surfactants decrease the zeta potential of nanoparticles due to a reduction in the thickness of the diffuse layer. Consequently, it has been proposed that to impart practical electrical properties on nanoemulsions, the electrostatic surfactants should be used in conjunction with stearic surfactants. In general, particles could be dispersed stably when the absolute value of zeta potential is above 30 mV due to the electric repulsion between particles. We found zeta potential values of the NEs in the range of 26.2- to -25.6 mV. This implies that the FBX-NEs prepared using solvent evaporation followed by probe sonication emulsification method would be a physically stable system.

Figure 7: Zeta potential graph of optimized formulation



Refractive Index

The refractive index value for the optimized formulation was found to be 1.43 ± 0.23 (mean \pm SD, n=3) which was compared with that of the water 1.44 ± 0.10 (mean \pm SD, n=3), no significant difference was found between both the values. The refractive index data prove the transparency of the system.

pH Determination

The pH of optimized nanoemulsion was determined with digital pH meter in the triplicate manner and it found 6.7 ± 0.589 to 7.2 ± 0.487 which is required for oral drug delivery.

Centrifugal stress measurement

1 mL aliquot of nanoemulsion was subjected to centrifugation at 12000 rpm for 10 min.

the creaming volume of each nanoemulsion was calculated by using formula and formulation were completed. No creaming or cracking of nanoemulsion found visually after study.

Determination of Viscosity

The viscosity of optimized nanoemulsion (F) was found 0.0159 ± 0.003 Pas (mean \pm SD, n=3). They are Non-Newtonian Liquids (viscosity decreases when the shear rate or shear stress increases) having Low viscosity values ensure easy handling and packing. Therefore, the viscosity of FBX-NE showed pseudo-plastic behaviour.

Drug Content by using UV spectroscopy

The drug content of the optimized batch was found to $87.23 \% \pm 0.896$ (mean \pm SD,

n=3). The optimum concentration of oil, surfactant, and co-surfactant was essential for maximum drug loading in the formulation to give maximum drug content of optimized batch. All formulation variables showed a significant effect on drug content.

Entrapment efficiency (EE%) of the FBX-NEs. 9 different batches of FBX-NEs were prepared by varying the lipid concentrations. The amount of drug was kept constant for all the batches. The entrapment efficiency of all the batches ranges from 74.2% to 86.6% respectively. Such a high value of entrapment efficiency may be due to the highly lipophilic nature of the drug FBX and its high solubility in Captex 200P. All values depicted in Table 5.

In-Vitro Study:
 The in-vitro release study for FBX-NE was

performed by the dialysis bag technique. In detail nanoemulsion containing 40mg drug was taken for the study. The study was conducted for 12 hr (2 hr in SGF and rest in SIF). The results were compared with the drug release from Febuxostat suspension (control) prepared using 0.4% w/v methylcellulose and the kinetics of drug release mechanism was studied. The FBX-NE and plain suspension were monitored for 2 hrs followed by SIF for 10 hrs. The result is shown in figure 18. From plain suspension, there was 15.38% drug release in 4 hrs and by end of 8 hrs, there was only 29.77% release. In the case of drug release from nanoemulsion formulation, there was a 69.86% drug release in 8 hrs and 93.61% by the end of 12 hrs. The Highest R^2 value 0.9945 values were obtained in Zero order Kinetic mode.

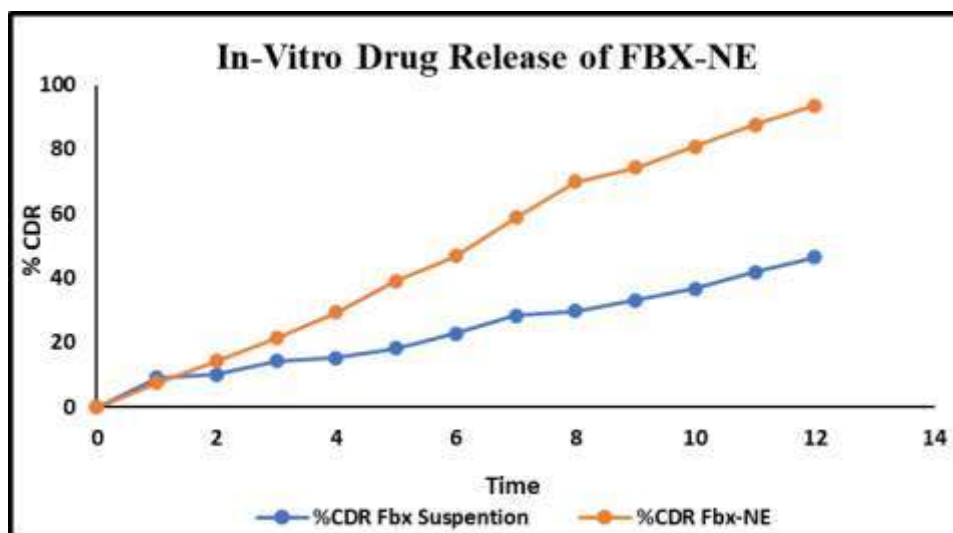


Figure 9: In-vitro drug release of FBX-NE

Table 8: In-vitro release profile of optimized batch

SrNo	Time(h)	%CDR
0	0	0
1	1	7.54464
2	2	14.3899
3	3	21.3883
4	4	29.3518
5	5	39.1312
6	6	46.8148
7	7	58.8293
8	8	69.8659
9	9	74.1967
10	10	80.7628
11	11	87.6083

12	12	93.6155
----	----	---------

A) Drug release kinetics

To study release kinetics, in vitro diffusion data obtained from optimized formulation were applied for various kinetics model viz. Zero order, first order, Higuchi release, and Korsmeyer-Peppas equation. Results are shown in Table 8.22. The zero order plot for batch NE showed in figure 8.19. The R² value was greater for zero order kinetic plots compared to other (First order, Higuchi) hence the nanoemulsion formulation follows zero order kinetic drug release profile i.e. the drug release rate is independent of its concentration. The pharmaceutical dosage forms following this profile release the same amount of drug by a unit of time and it is the ideal method of drug release to achieve a

pharmacological prolonged action. To confirm the exact mechanism of drug release kinetics from nanoemulsion formulation the data were fitted according to Korsmeyer-Peppas equation. When n takes the value of 0.5, it indicates the diffusion control drug release and for the value 1.0, it indicates swelling control drug release. Values of n between 0.5 to 1.0 can be regarded as indicates both phenomena (Anamoloustransport). The Korsmeyer-Peppas plot for batch FBX-NE showed in figure 8.22. The value of n in case of batch FBX-NE nanoemulsion formulation was suggested that the release of moxifloxacin from the nanoemulsion formulation followed the Anamoloustransport mechanism shows diffusion had an essential role in drug release.

Batch Code	Zero order (R ²)	First order (R ²)	Higuchi (R ²)	Korsmeyer-Peppas (R ²)	Best fitted model
FBX-NE	0.9945	0.7584	0.9151	0.8704	Zero order

Table 8.22 Kinetic model fitting of nanoemulsion formulation

AFM (Atomic Force Microscopy)

To determine the morphological properties and to confirm data obtained on droplet size and PDI by PCS. AFM was performed using AutoProbe CP- Research SPM (TM Microscopes-Bruker) with 90 μm large area scanners. Formulations were diluted with ultra-pure water 500 times (V/V), 10 μL of diluted sample was placed on circular mica and dried in vacuum. Due to the nature of the

samples, noncontact mode was applied. AFM measurements were performed in air, using noncontact probes Bruker Phosphorous doped silicon Tap300, with Al reflective coating and symmetric tip. Driving frequency of the cantilever was about 300 kHz. Both topography and "error signal" AFM images were taken and later analysed. The 3D image of AFM result was shown in fig.9.

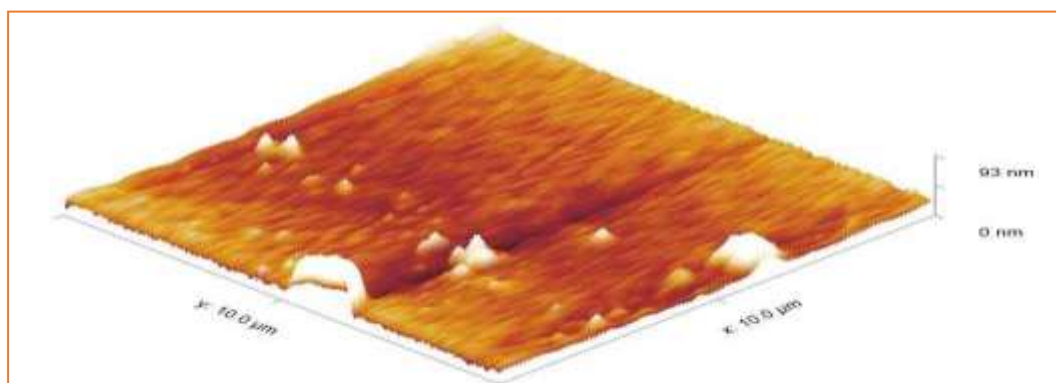


Figure 9: Atomic Force Microscopy of optimized FBX-NEs

HR-TEM (High Resolution Transmission Electron Microscopy):

High-resolution transmission electron microscopy (HR-

TEM) HR-TEM imaging of optimized FBX-NE was performed to observe the shape and size of the particle. The sample was prepared by mounting a single drop of FBX-NE dispersion on the carbon-coated copper grid which was stained by the

phosphotungstic acid (2 wt% negative stain) and uranyl acetate(1 wt% positive stain). After staining the sample was allowed to air dry for a few mins under room temperature and the image was captured by TEM (Jeol/JEM 2100) at a voltage 200 kV. The TEM imaging (Fig.9) showed the nanoparticles

were a nearly spherical shape with a smooth surface that appeared as a blackish spot. This study concluded with particle size well in agreement with DLS measurement with uniform distribution of particles.

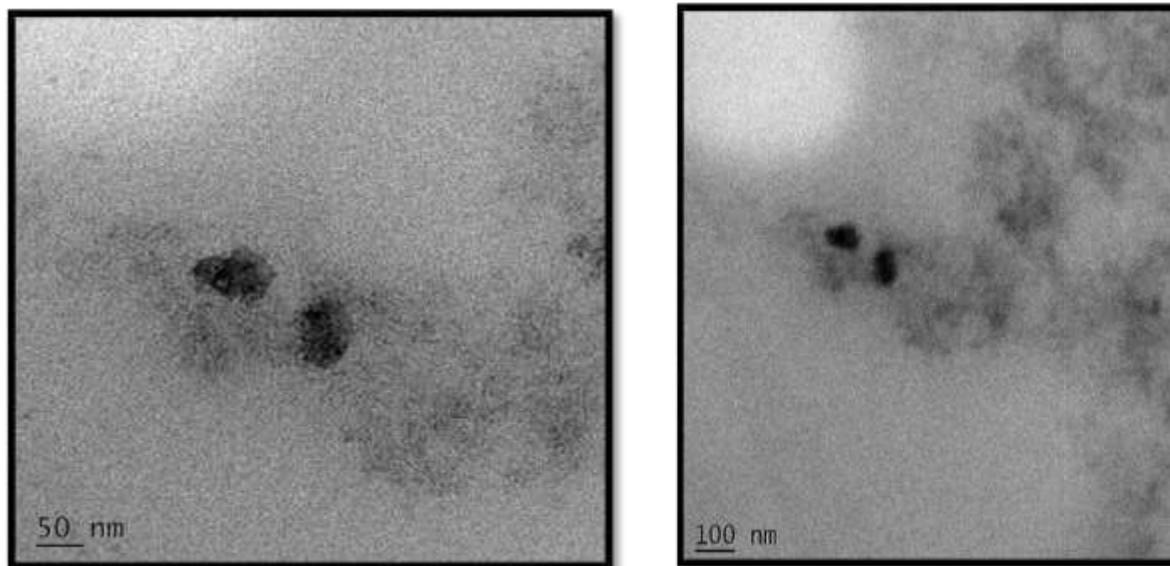


Figure 10 HR-TEM images of FBX-NE

Accelerated Stability Studies

Formulation showing optimum droplet diameter, PDI, and drug content (FBX) were selected for stability studies. According to ICH guidelines, optimized formulation was stored at 25 ± 2°C, 60 ± 5% RH. Formulations were evaluated at periodical

intervals of three months for various evaluation parameters which show that all results are in acceptable limits. The optimized batch shows that formulation can be stored well at room temperature (25°C)

Table 10: Stability studies

Parameter	Measurement on 1 st month		Measurement after 2 nd month		Measurement on after 3 rd month	
	4°C	25°C	4°C	25°C	4°C	25°C
Particle size	42.23±1.00	43.56±1.03	46.23±0.637	47.23±1.56	49.66±0.262	50.26±0.83
PDI	0.126±0.025	0.158±0.039	0.178±0.012	0.159±0.051	0.259±0.077	0.289±0.014
Zeta potential	-12.09±0.031	-13.03±0.559	-12.82±0.327	-12.82±0.244	-13.87±0.502	-13.59±0.350
Entrapment	90.6±0.236	85.66±0.15	77.69±0.891	89.76±	91.00±1.250	79.66±0.8

efficiency	8	0.789	97
------------	---	-------	----

IV. CONCLUSION

Febuxostat (FBX) is a novel drug that is developed for the treatment of gout and hyperuricemia. FBX is a weak acid (PKa 3.42) which is practically insoluble in water and the solubility was about 12.9 µg/ml in the water at 37 °C. The bioavailability of FBX is low and the half-life is about 5-8 hr. FBX is classified as a Biopharmaceutics Classification System (BCS) II drug due to its low solubility and high permeability. Hence, there is a need for formulating the Nanoparticles of the Febuxostat drug with suitable excipients and with fewer complications. Due to low water solubility FBX is having poor bioavailability. Here we increase the solubility of FBX with incorporating in various oils and it found higher in Captex 200 P oil and compatible with tween 80 and egg lecithin as a surfactant. The oil, surfactant, and co-surfactant concentration S-mix concentration was decided by plotting the pseudoternary phase diagram.

Full factorial design used for the optimization of the nanoemulsion batch with preparing 9 batches of formulation for further optimization of the batch.

For them to achieve higher bioavailability, the dissolution rate of the drug was enhanced by the synthesis of FBX-NE using probe sonication emulsification technique. The cumulative % drug release concerning time was found to 93.61% for the optimized batch. From the in vitro study, it became evident that enhancement in the bioavailability of FBX observed after drug loaded with nanoemulsion formulation. The microscopic study indicated a smooth surface and uniform size distribution. From the stability study of the formulation, it was found that the particle size and EE were not changed significantly. NEs were found to be stable for 3 months at 25 ± 2°C and 60 ± 5% RH.

The full factorial design proved to be successful in predicting the optimized formulation of FBX-NEs, based on particle size, Zeta potential, and entrapment efficiency. The optimized formulation produced nanoparticles with 74 nm in size with a narrow size distribution (PDI of 0.308), the zeta potential of -26.5 mV, and entrapment efficiency of 87%. In vitro release profiles of NEs indicated a burst release for the first 2 hrs followed by prolonged release profile for FBX

until about 12 hrs or more with the NE formulation.

REFERENCES:

- [1] S. Nazzal, I.I. Smalyukh, O.D. Lavrentovich, M.A. Khan, Preparation and in vitro characterization of a eutectic based semi solid self-nanoemulsified drug delivery system (SNEDDS) of febuxostat: Mechanism and progress of emulsion formation, *Int. J. Pharm.* 235(2002) 247–265. [https://doi.org/10.1016/S0378-5173\(02\)00003-0](https://doi.org/10.1016/S0378-5173(02)00003-0).
- [2] S. Ganta, M. Amiji, Co-administration of paclitaxel and curcumin in nanoemulsion formulations to overcome multidrug resistance in tumor cells, *Mol. Pharm.* 6 (2009) 928–939. <https://doi.org/10.1021/mp800240j>.
- [3] C. Liu, Z. Wang, H. Jin, X. Wang, Y. Gao, Q. Zhao, C. Liu, J. Xu, Effect of zymolysis and glycosylation on the curcumin nanoemulsions stabilized by β-conglycinin: Formation, stability and in vitro digestion, *Int. J. Biol. Macromol.* 142(2020) 658–667. <https://doi.org/10.1016/j.ijbiomac.2019.10.007>.
- [4] H.P. Thakkar, A. Khunt, R.D. Dhande, A.A. Patel, Formulation and evaluation of itraconazole nanoemulsion for enhanced oral bioavailability, *J. Microencapsul.* 00(2015) 1–11. <https://doi.org/10.3109/02652048.2015.1065917>.
- [5] S. Mahdi Jafari, Y. He, B. Bhandari, Nanoemulsion production by sonication and microfluidization - A comparison, *Int. J. Food Prop.* 9(2006) 475–485. <https://doi.org/10.1080/10942910600596464>.
- [6] N. Riquelme, R.N. Zúñiga, C. Arancibia, Physical stability of nanoemulsions with emulsifier mixtures: Replacement of tween 80 with quillaja saponin, *Lwt.* 111 (2019) 760–766. <https://doi.org/10.1016/j.lwt.2019.05.067>.
- [7] P. Fernandez, V. André, J. Rieger, A. Kühnle, Nano-emulsion formation by emulsion phase inversion, *Colloids Surfaces AP Physicochem. Eng. Asp.* 251(2004) 53–58. <https://doi.org/10.1016/j.colsurfa.2004.09.029>.
- [8] S. Sajjadi, Nanoemulsion formation by phase inversion emulsification: On the

- nature of inversion, *Langmuir*.22(2006)5597–5603. <https://doi.org/10.1021/la060043e>.
- [9] J.P.Gokhale, H.S.Mahajan, S.S.Surana, Quercetin loaded nanoemulsion-based gel for rheumatoid arthritis: In vivo and in vitro studies, *Biomed. Pharmacother.* 112(2019) 108622. <https://doi.org/10.1016/j.biopha.2019.108622>.
- [10] J. Hatanaka, H. Chikamori, H. Sato, S. Uchida, K. Debari, S. Onoue, S. Yamada, Physicochemical and pharmacological characterization of α -tocopherol-loaded nanoemulsions system, *Int. J. Pharm.* 396(2010)188–193. <https://doi.org/10.1016/j.ijpharm.2010.06.017>.
- [11] A.A. Date, M.S. Nagarsenker, Design and evaluation of self-nanoemulsifying drug delivery systems (SNEDDS) for cefpodoxime proxetil, *Int. J. Pharm.* 329(2007) 166–172. <https://doi.org/10.1016/j.ijpharm.2006.08.038>.
- [12] D. Mou, H. Chen, D. Du, C. Mao, J. Wan, H. Xu, X. Yang, Hydrogel-thickened nanoemulsion system for topical delivery of lipophilic drugs, *Int. J. Pharm.* 353(2008)270–276. <https://doi.org/10.1016/j.ijpharm.2007.11.051>.
- [13] M. Jaiswal, R. Dudhe, P.K. Sharma, Nanoemulsion: an advanced mode of drug delivery system, *3 Biotech.* 5(2015) 123–127. <https://doi.org/10.1007/s13205-014-0214-0>.
- [14] R.R. Bhosale, R.A. Osmani, P.P. Ghodake, S.M. Shaikh, S.R. Chavan, Nanoemulsion: A Review on Novel Profusion in Advanced Drug Delivery, *Indian J. Pharm. Biol. Res.* 2(2014)122–127. <https://doi.org/10.30750/ijpbr.2.1.19>.
- [15] M. Rosi Cappellani, D.R. Perinelli, L. Pescosolido, A. Schoubben, M. Cespi, R. Cossi, P. Blasi, Injectable nanoemulsions prepared by high pressure homogenization: processing, sterilization, and size evolution, *Appl. Nanosci.* 8(2018)1483–1491. <https://doi.org/10.1007/s13204-018-0829-2>.
- [16] H. Singh, S. Jindal, M. Singh, G. Sharma, I.P. Kaur, Nano-formulation of rifampicin with enhanced bioavailability: Development, characterization and in-vivo safety, *Int. J. Pharm.* 485(2015)138–151. <https://doi.org/10.1016/j.ijpharm.2015.02.050>.
- [17] A. Nagi, B. Iqbal, S. Kumar, S. Sharma, J. Ali, S. Baboota, Quality by design based silymarin nanoemulsion for enhancement of oral bioavailability, *J. Drug Deliv. Sci. Technol.* 40(2017)35–44. <https://doi.org/10.1016/j.jddst.2017.05.019>.
- [18] F. Gao, Z. Zhang, H. Bu, Y. Huang, Z. Gao, J. Shen, C. Zhao, Y. Li, Nanoemulsion improves the oral absorption of candesartan cilexetil in rats: Performance and mechanism, *J. Control. Release.* 149(2011)168–174. <https://doi.org/10.1016/j.jconrel.2010.10.013>.
- [19] E.S. El-leithy, H.K. Ibrahim, R.M. Sorour, In vitro and in vivo evaluation of indomethacin nanoemulsion as a transdermal delivery system, *7544(2013)1–8*. <https://doi.org/10.3109/10717544.2013.844742>.
- [20] P. Izquierdo, J. Esquena, T.F. Tadros, J.C. Dederen, J. Feng, M.J. Garcia-Celma, N. Azemar, C. Solans, Phase behavior and nanoemulsion formation by the phase inversion temperature method, *Langmuir*. 20(2004)6594–6598. <https://doi.org/10.1021/la049566h>.
- [21] R. Terkeltaub, J.S. Sundry, H.R. Schumacher, F. Murphy, S. Bookbinder, S. Biedermann, R. Wu, S. Mellis, A. Radin, The interleukin 1 inhibitor rilonacept in treatment of chronic gouty arthritis: Results of a placebo-controlled, monosequence crossover, non-randomised, single-blind pilot study, *Ann. Rheum. Dis.* 68(2009)1613–1617. <https://doi.org/10.1136/ard.2009.108936>.
- [22] M.R. Sherman, M.G.P. Saifer, F. Perez-Ruiz, PEG-uricase in the management of treatment-resistant gout and hyperuricemia, *Adv. Drug Deliv. Rev.* 60(2008) 59–68. <https://doi.org/10.1016/j.addr.2007.06.011>.
- [23] S. Singh, P. Parashar, J. Kanoujia, I. Singh, S. Saha, S.A. Saraf, Transdermal potential and anti-gout efficacy of Febuxostat from niosomal gel, *J. Drug Deliv. Sci. Technol.* 39(2017)348–361. <https://doi.org/10.1016/j.jddst.2017.04.020>.



- [24] N. Busso, A. So, Mechanisms of inflammation in gout, (2010).
- [25] S. Tiwari, H. Dwivedi, K.M. Kymonil, Urate crystal degradation for treatment of gout :a nanoparticulate combination therapy approach, (2015). <https://doi.org/10.1007/s13346-015-0219-1>.
- [26] M.E. Ernst, M.A. Fravel, Febuxostat: A selective xanthine-oxidase/xanthine-dehydrogenase inhibitor for the management of hyperuricemia in adults with gout, *Clin. Ther.* 31 (2009) 2503–2518. <https://doi.org/10.1016/j.clinthera.2009.11.033>.
- [27] J.E. Frampton, Febuxostat: A review of its use in the treatment of hyperuricaemia in patients with gout, *Drugs*. 75 (2015) 427–438. <https://doi.org/10.1007/s40265-015-0360-7>.
- [28] U. Asif, A.K. Sherwani, N. Akhtar, M.H. Shoaib, M. Hanif, M.I. Qadir, M. Zaman, Formulation Development and Optimization of Febuxostat Tablets by Direct Compression Method, *Adv. Polym. Technol.* 35 (2016) 1–7. <https://doi.org/10.1002/adv.21536>.